Advanced Synthesis & Catalysis

Accepted Article

Title: Combinatorial Mutation Analysis of ω-Transaminase to Create an Engineered Variant Capable of Asymmetric Amination of Isobutyrophenone

Authors: Hong-Gon Kim, Sang-Woo Han, and Jong-Shik Shin

To be cited as: *Adv. Synth. Catal.* 10.1002/adsc.201900184

Link to VoR: http://dx.doi.org/10.1002/adsc.201900184

10.1002/adsc.201900184

FULL PAPER

DOI: 10.1002/adsc.201((will be filled in by the editorial staff))

Combinatorial Mutation Analysis of ω-Transaminase to Create an Engineered Variant Capable of Asymmetric Amination of Isobutyrophenone

Hong-Gon Kim,[a] Sang-Woo Han[a] and Jong-Shik Shin[a,*]

[a] Department of Biotechnology, Yonsei University, Yonsei-Ro 50, Seodaemun-Gu, Seoul 03722, South Korea
[Phone: (+82)-2-2123-5884; Fax: (+82)-2-362-7265; e-mail: enzymo@yonsei.ac.kr]

Received: ((will be filled in by the editorial staff))

Supporting information for this article is available on the WWW under http://dx.doi.org/10.1002/adsc.201######.

Abstract. ω-Transaminase (ω-TA) is an important enzyme for asymmetric synthesis of chiral amines. Rapid creation of a desirable ω-TA variant, readily available for scalable process operation, is demanded and has attracted intense research efforts. In this study, we aimed to develop a quantitative mutational analysis (i.e., *R*-analysis) that enables prediction of combinatorial mutation outcomes and thereby provides reliable guidance of enzyme engineering through combination of already characterized mutations. To this end, we determined three mutatable active-site residues of ω-TA from *Ochrobactrum anthropi* (i.e., leucine 57, tryptophan 58 and valine 154) by examining activities of nine alanine-scanning mutants for seven substrate pairs. The *R*-analysis of the mutatable residues is based on assessment of changes in relative activities for a series of structurally analogous substrates. Using three sets of substrates (five α-keto acids, six arylalkylamines and three arylalkyl ketones), we found that combination of two point mutations display additive effects of each mutational outcome such as steric relaxation for bulky substrates or catalytic enhancement for amination of ketones. Consistent with the *R*-analysis-based prediction, the ω-TA variant harboring triple alanine mutations, i.e. L57A, W58A and V154A, showed high activity improvements for bulky substrates, e.g. a 3.2×10^4-fold activity increase for 1-phenylbutylamine. The triple mutant even enabled asymmetric amination of isobutyrophenone, carrying a branched-chain alkyl substituent to be accepted in a small binding pocket that normally shows a steric limit up to an ethyl group, with > 99 % *ee* of a resulting (*S*)-amine.

Keywords: ω-transaminase; chiral amines; asymmetric synthesis; protein engineering; combinatorial mutation

Introduction

Chiral amines are found in a number of pharmaceutical drugs as an essential building block,[1] which attracts extensive research efforts to develop chemocatalytic[2] and biocatalytic[3] methods for production of an enantiopure form. ω-Transaminase (ω-TA), more specifically amine transaminase or amine:pyruvate transaminase, is one of the competent workhorses available for asymmetric synthesis of the chiral amines starting with prochiral ketones and cheap amino donors such as isopropylamine and alanine.[4] Successful development of a scalable process using ω-TAs often depends on availability of a suitable enzyme for amination of a target ketone. This has invited huge research efforts aimed at engineering of native enzymes to endow desired properties such as altered substrate scope for bulky substrates and enhanced catalytic performance for amination of ketones.[5]

ω-TA exploits pyridoxal 5′-phosphate (PLP) as an internally bound cofactor to mediate amino group transfer from an amino donor (D) to an acceptor (A).[6] The whole catalytic cycle consists of two half reactions (Scheme 1); 1) oxidative deamination of an amino donor, accompanied by conversion of an enzyme-PLP form (E-PLP) to an enzyme form harboring pyridoxamine 5′-phosphate (PMP), and 2) reductive amination of an amino acceptor, leading to regeneration of E-PLP that resumes another catalytic cycle. Compared with α-transaminase responsible for amino group transfer exclusively between α-amino acids and α-keto acids, ω-TA displays a unique catalytic property that enables deamination of amines devoid of a carboxyl group and thereby amination of the resulting ketones and aldehydes as listed in Fig. 1.[5e,7] One of the important research goals in protein

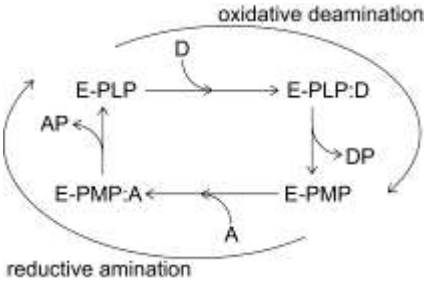

Scheme 1. A whole catalytic cycle of the ω-TA reaction. E-PLP:D and E-PMP:A represent Michaelis complexes. DP and AP stand for a deamination and an amination

product, respectively.

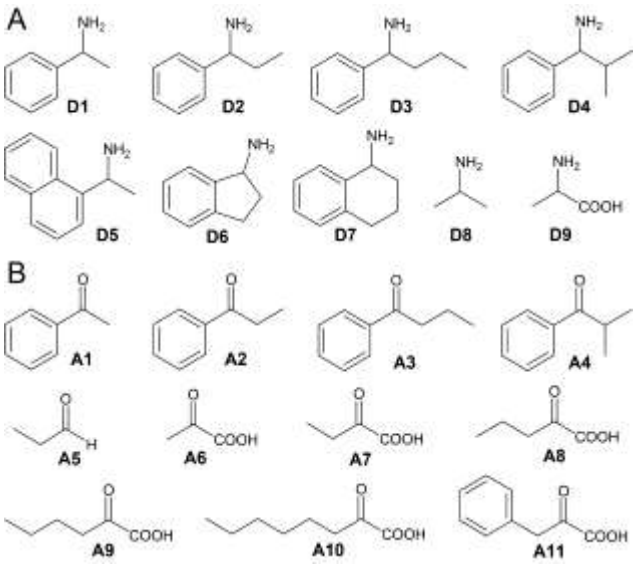

Figure 1. Substrates used in this study. (A) Amino donors and (B) amino acceptors.

engineering of ω-TAs is to increase a reaction rate for a target ketone, focusing on excavation of a narrow active site to facilitate productive binding of bulky ketones.[8]

Substrate scope of ω-TAs can be defined by a couple of general rules which were suggested by experimental data of quantitative substrate-activity relationship[7a] and then verified by structural modeling using substrate docking.[9] A two-binding-site model, consisting of a large (L) and a small (S) pocket, has successfully explained substrate specificity and stereoselectivity of most ω-TAs (Fig. 2).[4a,7a,10] First of all, the S pocket shows a strict steric limitation that denies entry of larger than an ethyl substituent. This feature has frustrated use of bulky substrates, attracting a great deal of protein engineering research to relieve the steric constraint.[8,11] Second, the L pocket can accommodate a hydrophobic as well as a carboxyl group. This dual recognition is mediated by an active site arginine that undergoes a gross movement depending on the type of a substituent that enters the L pocket.[6a,12] Third, ketones are very poor substrates even though their cognate amines are good substrates.[5d] For example, acetophenone (**A1**) shows a very low reactivity while its amination product, i.e. α-methylbenzylamine (**D1**), is a typical amino donor for most ω-TAs. Besides the steric issue in the S pocket, this is another crucial problem to be

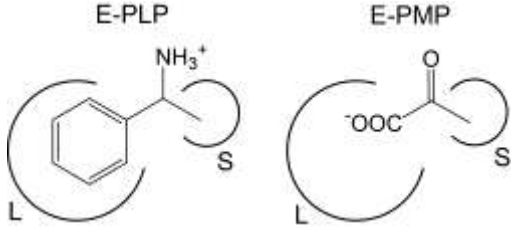

Figure 2. A two-binding-site model. α-MBA and pyruvate are depicted in the active site of E-PLP and E-PMP, respectively.

overcome for successful protein engineering in order to improve an enzyme activity for a given ketone.[5d,5e]

In the previous studies, we demonstrated that a single point mutation introduced in the active site of ω-TA could greatly alter enzyme properties.[5e,9e,13] For example, a single point mutation of tryptophan 58 in a (*S*)-selective ω-TA from *Ochrobactrum anthropi* (OATA) was proven to dramatically improve catalytic turnover of ketones.[5e] Moreover, OATA could be engineered to accept even a *n*-hexyl group of an α-keto acid in the S pocket by a point mutation of leucine 57.[13b] Nevertheless, we have not succeeded in creating an OATA variant capable of accommodating a branched-chain alkyl group in the S pocket although protein engineering to accept arylalkyl ketones carrying an isopropyl or a *t*-butyl group was reported elsewhere.[8b,11b] The aim of this study is the development of a predictive analysis tool for combinatorial mutations and its application to active site engineering of OATA that allows the accommodation of an isopropyl group in the S pocket and thus endows activities for (*S*)-**D4** and **A4**. Instead of mutant library generation and screening, we sought to develop a knowledge-guided strategy that was based on productive combination of single point mutations. The decision-making on whether or not to combine specific point mutations was guided by the proposed analysis tool that enabled quantitative interpretation of mutational effects and qualitative prediction of combinatorial mutation outcomes. Our strategy afforded rapid construction of an OATA variant showing activities for (*S*)-**D4** and **A4** through triple point mutations.

Results and Discussion

Development of a Knowledge-guided Strategy for Productive Combinatorial Mutations

Amino acid residues in the active site play a specific role to catalyze an enzyme reaction, which might be generally classified into two groups, i.e. the residues responsible for a binding step and the ones for a catalytic turnover step that are assessed by K_M and k_{cat} values, respectively. One of the difficult decisions to be made during protein engineering is how to select mutatable sites and how to predict productive combination of the beneficial and/or adverse point mutations that are identified in a previous step. As the number of point mutations increases, docking simulation results tend to be unreliable unless X-ray structures of intermediate-stage mutants are available. Therefore, those decisions often resort to cumulative hands-on experience and require time-consuming trial-and-error experimentation for library generation and screening.

The motivation of this study is to develop a knowledge-guided protein engineering strategy that exploits a predictive analysis tool for determining

productive combination of the mutatable residues. As outlined in Scheme 2, the proposed strategy starts with

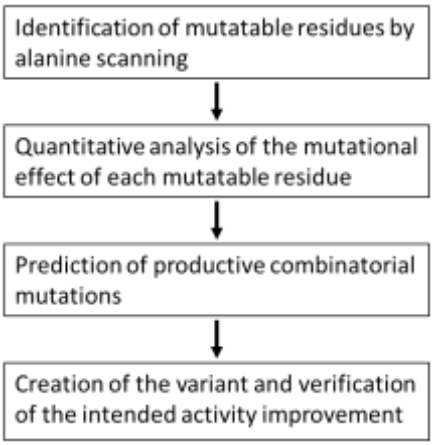

Scheme 2. Work flowchart of the proposed knowledge-guided protein engineering.

identification of mutatable residues to rule out detrimental mutations that are likely to cause a significant loss of desirable properties. This step is carried out by alanine scanning of the active site residues and activity measurements of the resulting mutants using representative substrate pairs. When the mutatable residues are determined, quantitative mutation analysis, i.e. *R*-analysis, is performed using a set of structurally related substrates, with a cosubstrate fixed, to probe whether the mutation site responds positively or negatively to the structural difference of a test substrate relative to a reference substrate. This analysis is based on comparison of relative reaction rates of the mutants to those of a wild-type enzyme. The next step is assessment of combinatorial mutation outcomes using the *R* values, enabling prediction of productive combination of point mutations. When the combinatorial mutation is determined, the final step is to verify the variant by activity measurement with a target substrate.

Native Activities for Representative Substrates

The two-binding-site model readily allows qualitative prediction of an enzyme activity of a native ω-TA for a given substrate pair. We determined relative activities of OATA for seven representative substrate pairs using (*S*)-**D1**/**A6** as a reference substrate pair (Table 1). Replacing **A6**, a typical amino acceptor for ω-TAs, with **A5** led to a similar activity, consistent with good activities of most ω-TAs for aldehyde.[9f] This property is in line with the steric constraint in the S pocket because the aldehydic hydrogen is the last one that might undergo steric hindrance in the S pocket. Moreover, the same steric consideration explains the drastic activity loss for **A8**, **A11** and (*S*)-**D3**. Although the substrate structure would not undergo rejection in the S pocket, **A1** shows a very low reactivity for most ω-TAs as also observed with 0.07 % activity of OATA for **A1** relative to that for **A6**. **D8** is regarded as an ideal amino donor for amination of ketones.[5a,14] However, not many ω-TAs display a significant activity for **D8**.[7a,15] The good activity of OATA for **D8** renders this enzyme attractive for practical synthesis of chiral amines, as mentioned elsewhere.[16]

The two-binding-site model is visualized with a X-ray structure of OATA, determined in a previous study,[5d] using docking models of (*S*)-**D1** and **A6** (Fig.

Table 1. Native enzyme activities of OATA for representative substrate pairs.[a]

Substrate pair	Specific reaction rate (v_i)[b] (mM min^{-1} mM-enzyme^{-1})	Relative activity[c] (%)
(*S*)-**D1**/**A6**	120 ± 25	100
(*S*)-**D1**/**A5**	114 ± 17	97
(*S*)-**D1**/**A8**	0.9 ± 0.2	0.7
(*S*)-**D1**/**A11**	n.r.[d]	< 0.5
(*S*)-**D3**/**A6**	n.r.	< 0.5
L-**D9**/**A1**	0.08 ± 0.01[e]	0.07
D8/**A6**	47 ± 20	39

[a] Reaction conditions: 10 mM amino donor, 10 mM acceptor and 2 μM enzyme.
[b] It represents an initial reaction rate per enzyme concentration.
[c] It is based on v_i for (*S*)-**D1**/**A6**.
[d] n.r.: not reactive (i.e., < 0.5 % of v_i for (*S*)-**D1**/**A6**).
[e] Due to low activities for ketones, high enzyme concentration (10 μM) was used for reliable measurement of the initial rate.

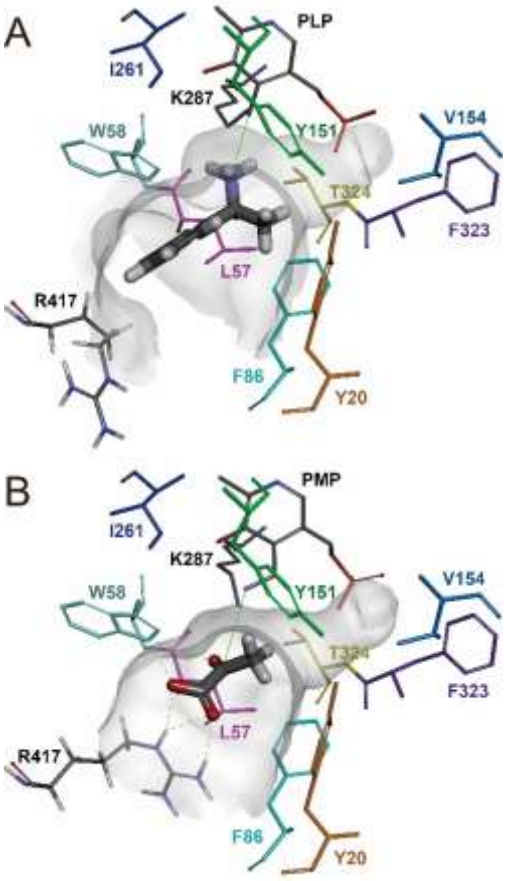

3). These docking poses represent typical productive

Figure 3. Docking models of (A) (*S*)-**D1** in E-PLP and (B) **A6** in E-PMP. Bound substrates are shown as thick sticks. The green solid lines represent (A) $N_{(S)\text{-}\mathbf{D1}}$–$C4'_{PLP}$ and (B) $C\alpha_{\mathbf{A6}}$–N_{PMP}. The green dotted lines represent hydrogen bonds. The active site is visualized by a Connolly surface. The L pocket is exposed to a solvent side and points toward a viewer.

substrate binding in the active site of ω-TA. Side chains of nine amino acid residues participate in the active site where arginine 417 acts as a conformational switch that controls the dual recognition mode. In contrast to arginine 417 involved in the substrate binding, lysine 287 play a pivotal role in catalytic turnover as a nucleophile and a Lewis acid/base. Note that OATA forms a homodimeric structure where the active site is located in the subunit interface and phenylalanine 86 and phenylalanine 323 come from the other subunit.

Identification of Mutatable Residues by Alanine Scanning

Using the active site model, we set out to determine which active site residues are amenable to engineering. This decision was made by eliminating the residues whose mutations led to significant loss of desirable activities, which was based on evaluation of activity changes of alanine scanning mutants that harbored a single alanine mutation of the nine active site residues. The resulting alanine mutants were subjected to activity measurements for the seven representative substrate pairs (Table 2). Relative activity less than 50 % of the wild-type enzyme was regarded as detrimental, shown in italic, whereas that over 150 % was considered as beneficial, shown in bold. Activity improvement over 10-fold was assigned as strongly beneficial and marked bold and underlined.

Three residues, tryptophan 58, valine 154 and isoleucine 261, showed beneficial activity changes for (*S*)-**D1**/**A6** by the alanine substitution. It is notable that the same mutants displayed activity improvements for L-**D9**/**A1** that is a substrate pair for the reverse reaction of (*S*)-**D1**/**A6**. Among the three mutations, W58A was strongly beneficial for L-**D9**/**A1** as reported previously.[5e] In addition, W58A was found to be the only alanine mutant showing a beneficial activity change for (*S*)-**D1**/**A5** whose amino acceptor is an aldehyde.

F86A caused a drastic activity loss for (*S*)-**D1**/**A6**, which led us to deter from measuring activities for other substrate pairs. Likewise, Y20A, Y151A, F323A and T324A turned out to be detrimental mutations for most substrate pairs. Despite beneficial activity changes for both (*S*)-**D1**/**A5** and L-**D9**/**A1**, I261A led to a drastic activity loss for **D8**/**A6**. Note that **D8** is one of the preferred amino donors for amination of ketones. Taken together, these six residues were crossed out from a list of mutatable residues.

For (*S*)-**D1**/**A8** and (*S*)-**D3**/**A6** pairs containing a substrate harboring a *n*-propyl group that exceeds the steric constraint of the S pocket, L57A elicited dramatic activity improvements for both substrate pairs owing to relocation of the S pocket as studied previously.[13] In addition, V154A led to an activity increase for (*S*)-**D1**/**A8**. Note that valine 154 closes the narrow S pocket tunnel as shown in Fig. 3 and thereby V154A leads to direct excavation of the S pocket. In line with this result, V153A of the ω-TA from *Paracoccus denitrificans* (PDTA) was observed to relieve the steric constraint in the S pocket.[9e] However, unlike PDTA, the steric relaxation was not observed for (*S*)-**D3**/**A6** with V154A of OATA. This result suggests that V154A might not attain steric relaxation strong enough to allow a detectable activity increase for (*S*)-**D3**/**A6**. It is intriguing that W58A showed a high activity increase for (*S*)-**D3**/**A6** but caused an adverse effect for (*S*)-**D1**/**A8**. The opposite mutational effects of W58A for **A8** and (*S*)-**D3** seem to be relevant to the type of substituents to be placed in the L pocket. Docking simulations predict that, unlike L57A, W58A leads a carbonyl oxygen of **A8** to form a hydrogen bond with arginine 417 and thereby renders the carbonyl carbon inaccessible to a nucleophilic attack by PMP (Fig. S1). In contrast, docking models showed productive binding of (*S*)-**D3** to both L57A and W58A (Fig. S1).

In the case of (*S*)-**D1**/**A11**, no mutant showed a

Table 2. Fold-changes in the activities of OATA caused by alanine mutation of the nine active site residues.[a]

Mutation	Fold-change in specific reaction rate ($r = v_{i,\,mutant}/v_{i,\,wild\text{-}type}$)[b]						
	(*S*)-**D1**/**A6**	(*S*)-**D1**/**A5**	(*S*)-**D1**/**A8**	(*S*)-**D1**/**A11**	(*S*)-**D3**/**A6**	L-**D9**/**A1**[f]	**D8**/**A6**
Y20A	*0.18 ± 0.14*	*0.15 ± 0.02*	0.69 ± 0.27	*n.r.*[c]	*n.r.*	*0.43 ± 0.03*	*0.40 ± 0.05*
L57A	1.07 ± 0.10	0.62 ± 0.06	**31.3 ± 0.7**	*n.r.*	> **17**[d]	0.58 ± 0.05	0.54 ± 0.21
W58A	**1.99 ± 0.31**	**1.80 ± 0.03**	*0.31 ± 0.14*	*n.r.*	> **23**[d]	**34.5 ± 4.5**	0.57 ± 0.28
F86A	*0.05 ± 0.01*	n.m.[e]	n.m.	n.m.	n.m.	n.m.	n.m.
Y151A	*0.39 ± 0.09*	*0.12 ± 0.06*	0.58 ± 0.37	*n.r.*	*n.r.*	*0.01 ± 0.001*	*0.07 ± 0.01*
V154A	**1.86 ± 0.53**	1.23 ± 0.16	**8.41 ± 0.61**	*n.r.*	*n.r.*	**1.65 ± 0.01**	1.26 ± 0.16
I261A	**1.60 ± 0.33**	0.80 ± 0.14	*0.25 ± 0.05*	*n.r.*	*n.r.*	**2.80 ± 0.01**	*0.05 ± 0.03*
F323A	*0.42 ± 0.14*	*0.46 ± 0.15*	*0.14 ± 0.05*	*n.r.*	*n.r.*	0.53 ± 0.04	*0.15 ± 0.07*
T324A	0.81 ± 0.16	*0.33 ± 0.26*	*0.10 ± 0.12*	*n.r.*	*n.r.*	*0.48 ± 0.01*	*0.07 ± 0.05*

[a] Font code for fold-changes: italic for $r < 0.5$, regular for $0.5 < r < 1.5$, bold for $r > 1.5$ and bold and underlined for $r > 10$.
[b] Reaction conditions: 10 mM amino donor and 10 mM acceptor.
[c] n.r.: not reactive (i.e., < 0.5 % of $v_{i,\ wild\text{-}type}$ for (*S*)-**D1**/**A6**).
[d] Owing to a non-detectable activity of the wild-type OATA under the reaction conditions, the minimum fold-change was estimated by dividing $v_{i,\ mutant}$ for (*S*)-**D3**/**A6** with 0.5 % of $v_{i,\ wild\text{-}type}$ for (*S*)-**D1**/**A6**.
[e] n.m.: not measured.
[f] The fold-change data for L-**D9**/**A1** were taken from a previous study.[5e]

Figure 4. Activity changes of OATA induced by either of L57A, W58A and V154A for three sets of substrates. (A) α-Keto acids with (*S*)-**D1** as an amino donor (both 10 mM), (B) (*S*)-arylalkylamines with **A6** as an acceptor (both 10 mM) and (C) arylalkyl ketones (50 mM) with **D8** (500 mM) as a donor in the presence of 15 % (v/v) DMSO.

detectable activity seemingly due to a too bulky size of the benzyl group of **A11** to enter the S pocket.

Taken all together, we chose leucine 57, tryptophan 58 and valine 154 as mutatable residues for further study. The alanine scanning results could be recapitulated as follows; 1) L57A elicits strong steric relaxation in the S pocket irrespective of the substituent type in the L pocket but does not achieve activity improvement for ketone, 2) W58A alleviates the steric constraint of a hydrophobic substrate and induces a dramatic activity improvement for ketone and 3) V154A leads to mild steric relaxation in the S pocket.

Activity Changes of the Three Alanine Mutants

To scrutinize precise mutational effects of the three mutatable residues, we examined activity changes of the three alanine mutants with three sets of substrates, i.e. α-keto acids (**A6**-**A10**), arylalkylamines (**D1**-**D3** and **D5**-**D7**), and arylalkyl ketones (**A1**-**A3**) (Fig. 4). Note that **A6**-**A10**, **D1**-**D3** and **A1**-**A3** carry *n*-alkyl side chains to be accommodated in the S pocket.

The wild-type OATA showed very low activities for α-keto acids carrying a side chain larger than an ethyl group, i.e. **A8**-**A10** (Fig. 4A). L57A showed high activity improvements for such bulky α-keto acids. Besides, V154A led to such improvements though in a lesser degree. In contrast, W58A did not engender the activity gain for **A8**-**A10**.

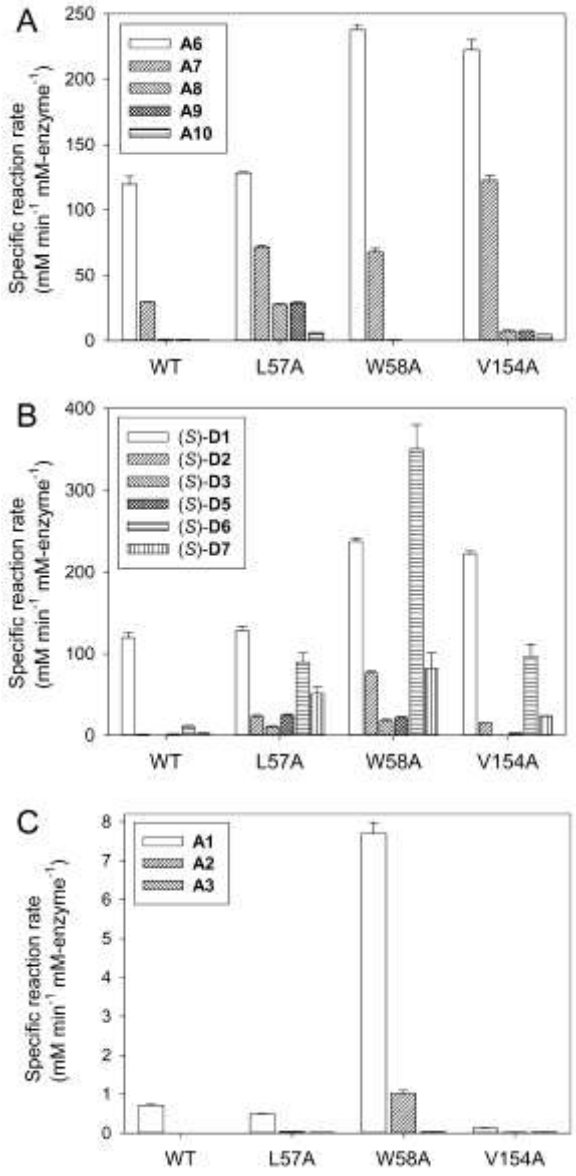

The steric constraint in the S pocket was observed to be more striking with **D1**-**D3** and the native activity was almost abolished even for **D2** carrying an ethyl group (Fig. 4B). The steric relaxation caused by L57A, as observed with α-keto acids, allowed activity improvements for **D2** and **D3** as well as for **D5**-**D7**. Similarly, activity improvements for the bulky arylalkylamines were observed with W58A. However, V154A did not induce such a beneficial effect for **D3** and **D5**.

In the case of arylalkyl ketones, W58A showed activity increases for all the three ketones (Fig. 4C). However, both L57A and V154A led to activity decreases for **A1** although a significant activity gain was found with **A2** and **A3**.

Theoretical Background of Quantitative Mutation Analysis

Fig. 4 enables direct activity comparison and thereby rapid determination of which mutation is the best for a given substrate pair. However, a crucial shortcoming of this is the inability to rule out contribution of a cosubstrate, used in the activity assay, from the mutational outcome. For example, Fig. 4A shows that V154A leads to an activity for **A7** 1.7-fold higher than L57A does. However, a similar activity increase for **A6** makes it ambiguous to conclude that V154A exerts a beneficial effect for **A7** stronger than L57A does because a part of the beneficial effect might come from an activity increase for (*S*)-**D1** used as an amino donor.

To clarify the ambiguity in the mutational analysis complicated by the contribution of a cosubstrate, we decided to develop a quantitative analysis method enabling elimination of the cosubstrate effect through normalization of relative activity of a mutant with that of a wild-type enzyme. For this analysis, we presume that the two half reactions, shown in Scheme 1, are independently affected by the active site mutation with a mutational scaling factor (i.e., *f*) relative to a wild-type enzyme, i.e. f_D and f_A for deamination and amination steps, respectively. As a result, mutational effect on an overall reaction rate ($v_{D,A}$) for a donor/acceptor (D/A) pair could be approximated to a product of the two *f* values as expressed in Eq. 1 where M and WT stand for a mutant and a wild-type, respectively.

$$(v_{D,A})_M = f_D f_A (v_{D,A})_{WT} \quad \text{(Eq. 1)}$$

We define relative activity (v_{rel}) for a D/A pair as $v_{D,A}$ divided by that for a reference substrate pair consisting of D_R and A_R.

$$v_{rel} = v_{D,A}/v_{D_R,A_R} \quad \text{(Eq. 2)}$$

Combining Eq. 1 and 2 leads to

$$(v_{rel})_M = \frac{f_D f_A}{f_{D_R} f_{A_R}} (v_{rel})_{WT} \quad \text{(Eq. 3)}$$

Because the reaction rates for different substrates in Fig. 4 were determined with a cosubstrate fixed, one of the mutational scaling factors in Eq. 3 can be cancelled out. For example, f_D is the same as f_{D_R} when using the activity data in Fig. 4A with (*S*)-**D1**/**A6** chosen as a reference substrate pair. As a result, Eq. 3 can be rearranged to give definition of the ratio of *f* values for amino acceptors (R_A).

$$R_A = \frac{f_A}{f_{A_R}} = \left.\frac{(v_{rel})_M}{(v_{rel})_{WT}}\right|_{\text{fixed amino donor}} \quad \text{(Eq. 4)}$$

Likewise, the activity data in Fig. 4B can be used to determine the ratio of *f* values for amino donors (R_D) as shown in Eq. 5.

$$R_D = \frac{f_D}{f_{D_R}} = \left.\frac{(v_{rel})_M}{(v_{rel})_{WT}}\right|_{\text{fixed amino acceptor}} \quad \text{(Eq. 5)}$$

The *R* value represents how much the mutation is beneficial for a target substrate relative to a reference substrate. Therefore, the *R* value can be interpreted as whether the mutation responds positively or negatively to the structural difference of a target substrate compared to a reference. Consequently, the *R* value over unity indicates a beneficial mutational effect on the change in the substrate structure whereas $0 < R < 1$ indicates an adverse effect. As a result, the *R*-analysis can be used to provide a quantitative

measure of the mutational effect on the structural difference of substrates.

R-Analysis of the Single Point Mutations

Using Eq. 4 or Eq. 5, the *R*-analysis was carried out with specific reaction rate data in Fig. 4 (Table 3). The *R*-analysis with **D3**, **A2** and **A3** was not possible because the activities of the wild-type OATA for these substrates were lower than a detection limit under the assay conditions. The *R* value of L57A is 2.3 for **A7** but becomes much larger as the size of the side chain

Table 3. *R*-analysis of the three single point mutations.[a]

Substrate	*R*		
	L57A	W58A	V154A
A7	2.3 ± 0.1	1.2 ± 0.1	2.2 ± 0.2
A8	29.1 ± 7.4	0.3 ± 0.1	4.5 ± 1.2
A9	30.4 ± 4.6	0.0	4.6 ± 0.7
A10	11.5 ± 0.8	0.0	5.2 ± 0.4
(*S*)-**D2**	14.4 ± 1.5	25.8 ± 2.2	5.6 ± 0.5
(*S*)-**D5**	12.4 ± 1.3	6.0 ± 0.5	0.9 ± 0.1
(*S*)-**D6**	7.5 ± 1.2	15.7 ± 1.9	4.6 ± 0.8
(*S*)-**D7**	17.6 ± 3.2	15.2 ± 3.8	4.7 ± 0.5

[a] The reference substrate pair is (*S*)-**D1**/**A6**.

of α-keto acid exceeds an ethyl group (**A8**-**A10**). The similar *R* values of L57A for **A8** and **A9** suggest that *n*-propyl and *n*-butyl substituents undergo a similar degree of steric relaxation in the S pocket. A 2.5-fold decrease in the *R* value for **A10**, compared to those for **A8** and **A9**, indicates that the steric relaxation induced by L57A becomes less favorable for a *n*-hexyl group. The steric relaxation by L57A leads to high *R* values for arylalkylamines. It is notable that the *R* value for (*S*)-**D5** is similar to that for (*S*)-**D2** although a structural difference between (*S*)-**D5** and a reference amino donor ((*S*)-**D1**), unlike between (*S*)-**D2** and (*S*)-**D1**, lies in the substituent that enters the L pocket. This result is consistent with the previous investigation that the steric relaxation in the S pocket induced by L57A comes from relocation of the S pocket caused by the expansion of the L pocket.[13a]

In contrast to L57A, the *R* values of W58A for **A8**-**A10** were much lower than unity. This results clearly indicate that W58A is detrimental to enzyme activity for α-keto acid carrying a side chain larger than an ethyl group. However, the adverse mutational effect of W58A turns into a beneficial one for arylalkylamines as good as that of L57A.

V154A leads to the *R* values higher than unity up to 5.6, indicating mild steric relaxation compared to L57A and W58A. It is notable that the *R* value for (*S*)-**D5** is close to unity, indicating that V154A benefits the enzyme activities for (*S*)-**D5** and (*S*)-**D1** by the same degree. This result suggests that V154A does not tell a structural difference of the substituents placed in the L pocket and attains the mild steric relaxation purely by excavation in the S pocket.

R-Analysis of the Double Point Mutations

The *R*-analysis enabled quantitative assessment of the steric relaxation induced by each point mutation depending on the substrate type. Although we could not perform the *R*-analysis with ketones, W58A was found to elicit dramatic activity improvements for **A1** and **A2** (Fig. 4C). Keeping these results in mind, we decided to tackle an intriguing question: what does combination of two point mutations lead to in terms of an additive effect? To address this, we constructed three combinatorial mutants and carried out activity measurements with the three sets of substrates (Fig. 5). Note that L57A/W58A is proximal mutations whereas L57A/V154A and W58A/V154A are distal mutations.

For **A6** and **A7**, the two double mutants harboring W58A showed higher activities than the L57A/V154A mutant did (Fig. 5A). However, an opposite trend was observed for **A8**-**A10**. This result is ascribable to the adverse effect of W58A for **A8**-**A10**. It is notable that activity increases for **A8**-**A10** induced by L57A/ V154A are larger than those induced by each point mutation. For example, activity of the L57A/V154A mutant for **A10** is 3.5 and 8.2-fold higher than those of L57A and V154A mutants, respectively. Taken together, enzyme activities of the double mutants for bulky α-keto acids showed additive effects of each point mutation, i.e. strongly beneficial by L57A,

Figure 5. Enzyme activities of OATA variants, carrying double mutations, for three sets of substrates. (A) α-Keto acids, (B) (*S*)-arylalkylamines and (C) arylalkyl ketones.

weakly beneficial by V154A and strongly detrimental by W58A.

The additive effect was also observed with arylalkylamines (Fig. 5B). However, as indicated by the *R*-analysis in Table 3, W58A exhibited a strongly positive effect on the steric relaxation for the arylalkylamines. As a result, the L57A/W58A mutant showed the highest activity for (*S*)-**D2**, (*S*)-**D3** and (*S*)-**D5** among the three double mutants. For (*S*)-**D6** and (*S*)-**D7**, the two double mutants harboring W58A displayed similar activities which were higher than those of the L57A/V154A mutant.

For ketones, W58A exhibited a strongly beneficial effect as shown in Fig. 4. Consistent with this result the two W58A-bearing mutants displayed activities for **A1** and **A2** much higher than the L57A/V154A mutant did (Fig. 5C). It is notable that L57A/W58A led to an impressive activity improvement for **A3** whereas W58A/V154A failed to induce such an increase, consistent with the steric relaxation in the S pocket by L57A stronger than that by V154A as observed before.

To quantify the combinatorial mutation effects, we

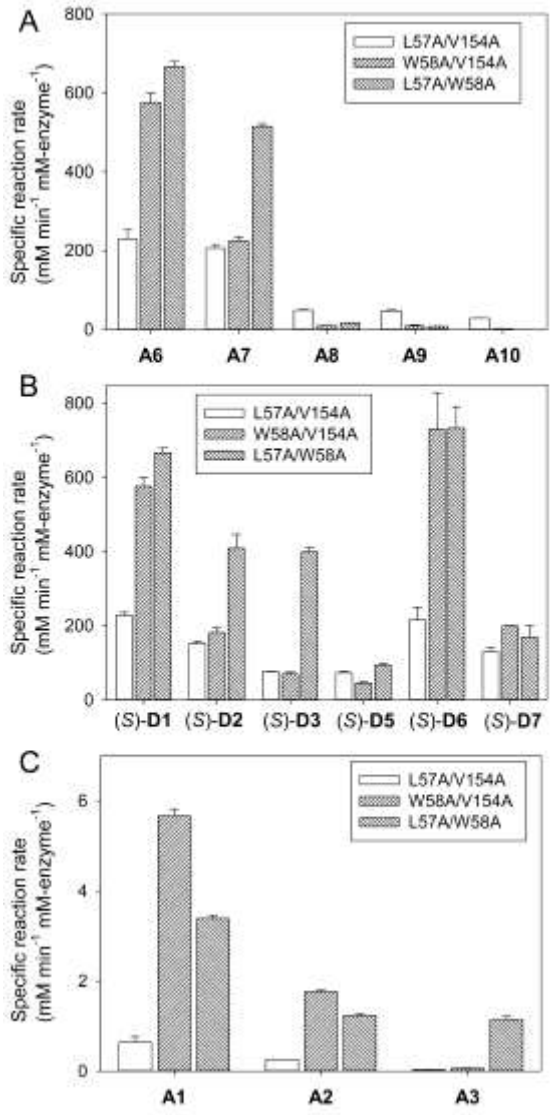

Table 4. *R*-analysis of the variants carrying double mutations.[a]

Substrate	*R*		
	L57A/W58A	L57A/V154A	W58A/V154A
A7	3.1 ± 0.2	3.7 ± 0.5	1.6 ± 0.1
A8	3.2 ± 0.8	28.8 ± 8.0	2.2 ± 0.6
A9	1.6 ± 0.3	28.2 ± 5.3	2.1 ± 0.3
A10	0.04 ± 0.01	31.3 ± 3.9	0.9 ± 0.1
(*S*)-**D2**	49.4 ± 6.0	53.8 ± 5.0	25.5 ± 2.9
(*S*)-**D5**	9.1 ± 0.9	21.1 ± 2.1	5.1 ± 0.6
(*S*)-**D6**	11.7 ± 1.4	10.0 ± 1.9	13.5 ± 2.2
(*S*)-**D7**	11.2 ± 2.3	25.1 ± 3.2	15.2 ± 1.6

[a] The reference substrate pair is (*S*)-**D1**/**A6**.

carried out the *R*-analysis of the double mutants (Table 4). Owing to the adverse effect of W58A for bulky α-keto acids, the two W58A-bearing mutants led to *R* values for **A8**-**A10** lower than those of L57A or V154A single mutants. In contrast, L57A/V154A led to high *R* values for the bulky α-keto acids. The *R* values of the L57A/V154A mutant for **A8** and **A9** were not very different from those of the L57A mutant, indicating that V154A does not make additional contribution to the steric relaxation achieved by L57A for *n*-propyl and *n*-butyl groups. However, L57A/V154A attains a synergic effect for **A10** carrying a bulkier side chain, leading to 2.7 and 6-fold increases in the *R* values relative to those of L57A and V154A, respectively. It is notable that the synergic effect was found with the L57A/V154A mutant for all the four arylalkylamines. Such a synergic effect was also observed for (*S*)-**D2** with L57A/W58A.

R-based Prediction of Triple Mutation

Based on the *R*-analysis results so far, we examined whether the *R*-analysis could be used to predict mutational outcome of the variant harboring triple mutation. For α-keto acids, an adverse effect of W58A was observed for bulky substrates in alone as well as in combination with L57A or V154A. Unfortunately, the *R*-analysis is not available to predict what mutational outcome is caused by addition of W58A to a L57A/V154A double mutant. Instead, the *R*-analysis would allow quantitative evaluation of the mutational effects of L57A and V154A for bulky α-keto acids on a W58A background. To this end, we carried out a modified *R*-analysis in which the W58A mutant served as a parental enzyme (Table 5). As a result, *R*-analysis was carried by normalizing relative activities of the

Table 5. A modified *R*-analysis of double mutants for α-keto acids using the W58A mutant as a parental enzyme.[a]

Substrate	*R*	
	L57A/W58A	W58A/V154A
A7	2.7 ± 0.1	1.4 ± 0.1
A8	12.0 ± 3.3	8.1 ± 2.2

[a] The reference substrate pair is (*S*)-**D1**/**A6**.

Table 6. A modified *R*-analysis of double mutants for ketones using the W58A mutant as a parental enzyme.[a]

Substrate	*R*	
	L57A/W58A	W58A/V154A
A2	2.8 ± 0.3	1.8 ± 0.1
A3	76.0 ± 6.2	2.5 ± 0.2

[a] The reference substrate pair is **D8**/**A1**.

L57A/W58A and W58A/V154A mutants with that of the W58A mutant. Owing to the non-detectable activities of W58A for **A9** and **A10**, *R*-analysis was performed only with **A7** and **A8**. The *R*-analysis suggests that addition of L57A or V154A to W58A would lead to a weak beneficial effect for **A7** as observed with the *R*-analysis of L57A and V154A on a wild-type enzyme in Table 3. In contrast, both mutations were predicted to confer stronger beneficial effects for **A8** to the W58A mutant similarly to the wild-type enzyme shown in Table 3. Therefore, the modified *R*-analysis suggests that the beneficial

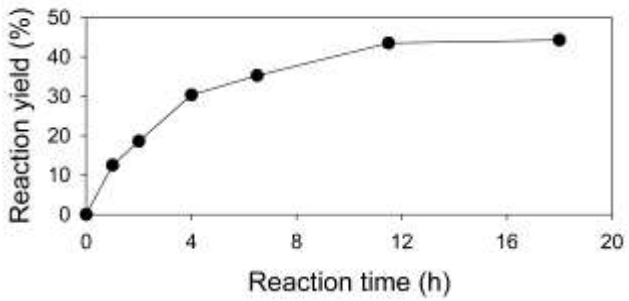

effects of L57A and V154A for bulky α-keto acids are conserved even after the adverse W58A mutation.

For arylalkylamines, we found that all the three double mutants led to beneficial mutational effects and showed high *R* values. Therefore, the triple mutant is expected to display enzyme activities for the bulky amines higher than all the double mutants.

For ketones, we could not determine the *R* values of the single point mutations because of too low activities of the wild-type enzyme for **A2** and **A3**. However, Fig. 4C and 5C indicate that W58A is a strong driver for enhancing activities for ketones while L57A and V154A are hard to be evaluated. To clarify the mutational effects of L57A and V154A for ketones, we carried out again the modified *R*-analysis using the W58A mutant as a parental enzyme (Table 6). The two W58A-bearing double mutants show similar *R*-values for **A2**, suggesting that both L57A and V154A would lead to a weak beneficial effect on steric relaxation for **A2** relative to **A1**. The *R*-values for **A3** suggest a strongly and a weakly beneficial effect of L57A and V154A, respectively, on enzyme activity of the W58A mutant for **A3** relative to **A1**. In addition to the high *R* value of L57A/W58A for **A3**, the *R* value of W58A/ V154A higher than unity led us to posit that addition of both mutations to the W58A mutant would be worth trying to improve activities for bulky ketones.

Motivated by the *R*-based prediction for bulky amines and ketones, we prepared the triple mutant carrying L57A/W58A/V154A and measured the enzyme activities for various substrates in comparison with the three double mutants (Table 7). The additive effect of the three point mutations was remarkable to confer dramatic activity improvements for bulky substrates (i.e., **A8**-**A10**, **D2**-**D3**, **D5**-**D7** and **A2**-**A3**) to a wild-type enzyme. For example, the triple mutant achieved 550, 32000 and over 790-fold activity increases for **A8**, **D3** and **A3**, respectively, compared to a wild-type enzyme. It is notable that the triple mutation led to activities for **A8** and **A9** higher than those of the L57A/V154A variant. Likewise, it is notable that the triple mutation led to a 2.5-fold activity improvement for **A3** relative to L57A/W58A.

Table 7. Activity improvement of the triple mutant.

Substrate	Specific reaction rate[a] (mM min^{-1} mM-enzyme^{-1})	Fold-change relative to 57/58, 57/154, 58/154[b]
α-Keto acids		
A6	709 ± 3 (6)[c]	1.1, 3.1, 1.2
A7	556 ± 38 (19)	1.1, 2.7, 2.5
A8	487 ± 26 (550)	30.8, 10.0, 52.7
A9	297 ± 49 (340)	38.2, 6.2, 33.4
A10	28 ± 3 (58)	228.6, 1.0, 13.3
Arylalkylamines		
(*S*)-**D1**	709 ± 3 (6)	1.1, 3.1, 1.2
(*S*)-**D2**	741 ± 32 (500)	1.8, 4.9, 4.1
(*S*)-**D3**	777 ± 10 (32000)	1.9, 10.2, 11.1
(*S*)-**D5**	314 ± 11 (170)	3.4, 4.3, 7.0
(*S*)-**D6**	993 ± 31 (88)	1.4, 4.6, 1.4
(*S*)-**D7**	308 ± 18 (110)	1.8, 2.4, 1.5
Ketones		
A1	3.41 ± 0.08 (5)	1.1, 5.3, 0.6
A2	3.86 ± 0.05 (> 1100)[d]	3.1, 14.7, 2.2
A3	2.83 ± 0.02 (> 790)[d]	2.5, 88.6, 45.9

[a] Reaction conditions were the same as those in Fig. 4.
[b] Fold-changes represent a reaction rate of the L57A/W58A/V154A mutant relative to those of L57A/W58A, L57A/V154A and W58A/V154A mutants.
[c] The number in parenthesis represents a fold-change in the specific reaction rate relative to that of the wild-type enzyme.
[d] Due to non-detectable activities of the wild-type enzyme for **A2** and **A3**, the minimum fold-change was based on the detection limit (i.e., 0.5 % activity of the wild-type enzyme for **A1**).

Asymmetric Synthesis of (*S*)-D4

To examine how much the triple mutation allows steric relaxation for bulky substrates, we tested (*S*)-**D4** as a probe substrate. Single point mutations did not engender a measurable activity for (*S*)-**D4**. The triple mutant showed a specific reaction rate of 86 ± 2 mM min^{-1} mM-enzyme^{-1}, at 20 mM *rac*-**D4** and 10 mM **A6** which corresponds to 5, 23 and 41-fold activity gains relative to those of L57A/W58A, L57A/V154A and W58A/V154A mutants, respectively. The activity of the triple mutant for (*S*)-**D4** corresponds to even 72 % activity of a wild-type enzyme for (*S*)-**D1**. Docking simulation suggests that the expanded active site induced by the triple mutation allows productive binding of (*S*)-**D4** in a way different from that of (*S*)-**D1** in the wild-type active site (Fig. S2). The high activity for (*S*)-**D4** encouraged us to test **A4** as an amino acceptor. Among all the OATA mutants used in this study, the triple mutant was the only one that allowed a measurable activity for **A4**, i.e. specific reaction rate = 0.06 ± 0.01 mM min^{-1} mM-enzyme^{-1} at 50 mM **A4** and 500 mM **D8**.

To demonstrate synthetic utility of the triple mutant, we carried out analytical-scale synthesis of (*S*)-**D4** at 15 % (v/v) DMSO under ambient pressure (Fig. 6).

Figure 6. Asymmetric synthesis of (*S*)-**D4** using the triple mutant. Reaction conditions were 5 mM **A4**, 500 mM **D8**, 100 μM triple mutant and 15 % (v/v) DMSO at 1 atm. Reaction yield is based on the produced (*S*)-**D4** analyzed by HPLC.

Note that DMSO is a popularly used cosolvent to increase solubility of hydrophobic ketones used as a

substrate for ω-TA reactions. Reaction yield reached 44 % at 11.5 h and then leveled off seemingly because the reaction approached a thermodynamic limit. The enantiopurity of the resulting (*S*)-**D4** was over 99 % *ee*.

Encouraged by the analytical-scale result, we moved on to preparative-scale asymmetric synthesis of (*S*)-**D4** using the triple mutant. To this end, we decided to increase the DMSO content owing to the low solubility of **A4** in water. Solubility of **A4** was measured at 0 - 50 % (v/v) DMSO content, showing gradual solubility increases from 5.5 mM up to 41.5 mM at 50 % DMSO (Fig. S3). Considering that cosolvent is usually detrimental to enzyme stability, we examined how the varying DMSO contents affected amination of 100 mM **A4** with 500 mM **D8** at 10 - 50 % (v/v) DMSO (Fig. 7). Note that **A4** beyond the solubility forms emulsion under the DMSO contents. Reaction progress became higher up to 30 % DMSO seemingly owing to the solubility increases. However, the reaction progress was slowed down as the DMSO content exceeded 30 % and eventually led to a drastic decease at 50 %. These results suggest that enzyme inactivation

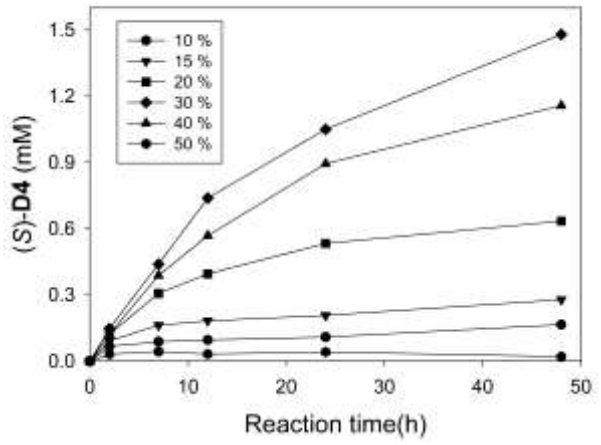

Figure 7. Effect of the DMSO content on the asymmetric amination of **A4**. Reaction conditions were 100 mM **A4**, 500 mM **D8**, 10 μM triple mutant and 10 - 50 % (v/v) DMSO at 1 atm.

caused by DMSO would overwhelm the gain in the reaction rate by the solubility increase as the DMSO content becomes higher than 30 %.

Based on the reaction progress results above, we performed a 50-mL preparative-scale reaction at 50 mM **A4**, 500 mM **D8**, 100 μM triple mutant and 30 % (v/v) DMSO under reduced pressure (i.e., 0.6 bar) for equilibrium shift by removing volitile acetone. After 46-h reaction, reaction yield reached 45.6 % and the enatiopurity of the produced (*S*)-**D4** was > 99 % *ee*. It is notable that enzyme stability was remarkably high during the preparative-scale reaction and less than 10 % activity loss was detected at the end of the reaction (data not shown). Product isolation was carried out using cation-exchange chromatography, leading to 86 mg (*S*)-**D4** (51 % recovery yield). The isolated (*S*)-**D4** was structurally characterized by ^{1}H NMR, ^{13}C NMR and LC/MS (see Supporting information).

Conclusion

Rapid creation of a desirable ω-TA variant is crucial to successful process development for asymmetric amination of a target ketone. In this study, we demonstrated that combinatorial mutation of active site residues, aided by *R*-analysis for quantitative assessment of mutational effects, allowed such a rapid construction of a desirable variant capable of accepting even an isopropyl group in the S pocket of OATA. We found that the mutatable residues of OATA exhibit additive effects of enzyme properties, affording prediction of combinatorial mutation outcomes for bulky amines and ketones. However, the *R*-analysis has a limitation in predicting mutational outcomes when combining beneficial and detrimental mutations as illustrated with bulky α-keto acids. Nevertheless, the practical utility of the proposed approach is that it does not require time-consuming library construction and screening but instead exploits prior knowledge on mutational effects of the active site residues. Considering a very low activity of a wild-type ω-TA for a target ketone in most cases, the *R*-analysis would better be performed with a cognate amine and then test the combinatorial mutation with the target ketone.

Experimental Section

Chemicals

(*S*)-**D3**, **A3** and **A5** were purchased from Alfa Aesar (Ward Hill, MA, USA). **D4** was purchased from Enamine Ltd. (Kiev, Ukraine). **D8** and L-**D9** were obtained from Junsei Chemical Co. (Tokyo, Japan) and Acros Organics Co. (Geel, Belgium), respectively. Methanol, acetonitrile, DMSO and perchloric acid were obtained from Duksan Pure Chemicals Co. (Ansan, South Korea). All other chemicals were purchased from Sigma-Aldrich Co. (St. Louis, MO, USA). Materials used for preparation of culture media were obtained from Difco (Spark, MD, USA).

Site-directed mutagenesis

Mutagenesis was carried out using a QuikChange Lightning site-directed mutagenesis kit (Agilent Technologies Co.) according to an instruction manual. All the nine alanine scanning mutants and the double mutant carrying L57A/ W58A were constructed in our previous studies.[5d,13b] The three mutants carrying L57A/V154A, W58A/V154A and L57A/W58A/V154A mutations were generated by V154A substitution of L57A, W58A and L57A/W58A mutants, respectively, as templates. The V154A substitution was carried out using a forward (5′-CGGCTATCACGGTGCG ACGATTGCCTCTG-3′) and a reverse primer (5′-CAGAG GCAATCGTCGCACCGTGATAGCCG-3′). Mutagenesis was confirmed by DNA sequencing.

Protein expression and purification

Escherichia coli BL21(DE3) cells transformed with a pET28a(+) expression vector harboring a OATA gene were used for protein expression. Cultivation of *E. coli* BL21(DE3) cells, overexpression of the His_6-tagged ω-TAs and protein purification were carried out as described elsewhere.[5d] Molar concentrations of the purified ω-TAs were determined by measuring UV absorbance at 280 nm. Detailed information on the expression plasmids and molar extinction coefficients is shown in Table S1.

Enzyme assay

All the enzyme assays were carried out at pH 7 (50 mM potassium phosphate buffer) in a water bath set to 37 °C. Enzyme activities for α-keto acids (i.e., **A6**-**A11**) were measured at 10 mM amino acceptor and 10 mM (*S*)-**D1**. Typical reaction volume was 100 μL. The reaction was allowed for 10 min and then stopped by adding 600 μL acetonitrile. Protein precipitate was removed by centrifugation (13,000 rpm, 10 min) and the supernatant was subjected to HPLC analysis of the produced **A1**. The reaction conditions for measurement of enzyme activities for amines (i.e., **D1**-**D7**) were 10 mM (*S*)-amine (or 20 mM racemic amine for **D4**, **D6** and **D7**) and 10 mM **A6**. Produced ketones were analyzed by HPLC.

To measure activities of ω-TAs for arylalkyl ketones (i.e., **A1**-**A4**), enzyme reactions were conducted at 50 mM ketone and 500 mM **D8** in the presence of 15 % (v/v) DMSO. Typical reaction volume was 0.4 mL. To obtain the initial rates, aliquots (typically 20 μL) of the reaction mixture were taken after 1 h and mixed with 380 μL of 4.4 % (v/v) $HClO_4$ solution to stop the reaction. After centrifugation, the resulting supernatant was subjected to chiral HPLC for analyses of produced amines.

Molecular modeling

Molecular modeling was carried out using a Discovery Studio package (version 3.5.0, Accelrys) as described previously with minor modifications.[5d] Docking simulations of α-keto acid and arylalkylamine were performed with an E-PMP structure harboring an inward conformation of an active site arginine (E-PMP_{in}) and an E-PLP structure harboring an outward-pointing arginine (E-PLP_{out}), respectively. A crystal structure of OATA (PDB ID: 5GHF)[5d] corresponds to E-PMP_{in} and thus could be directly used for docking simulation of α-keto acid. For docking simulation of arylalkylamines, the E-PLP_{out} structure of OATA was constructed by structural replacement of arginine 417, lysine 287 and PMP of the E-PMP_{in} structure of OATA with arginine 415 and internal aldimine of the E-PLP_{out} structure of PDTA (PDB ID: 4GRX)[17] whose sequence identity is 41 % with OATA.[13b] First, coordinates of lysine 287 and PMP of 5GHF were substituted by those of the internal aldimine of 4GRX after parallel translation of coordinates where C_α of the catalytic lysine of 4GRX coincided with that of 5GHF. To render the transported internal aldimine closer to a catalytically competent structure, hybridization states of the C4′ and N atoms were changed to sp^2. Hydrogen bonds in a phosphate binding cup, i.e. formed between the phosphate group of the cofactor and G118/S119/T324, were found to be conserved after the structural replacement. Second, coordinates of arginine 417 of 5GHF were replaced by those of arginine 415 of 4GRX following the same procedures. Structural models of OATA mutants were prepared by alanine substitution of the mutation sites of the wild-type structure. Docking simulations were performed using a CDOCKER module under a default setting (i.e., 2000 steps at 700 K for a heating step, 5000 steps at 300 K for a cooling step and 8 Å grid extension).

Asymmetric synthesis of (*S*)-D4

Asymmetric synthesis of (*S*)-**D4** was performed in a 50 mM Tris buffer (pH 9.0) at 37 °C and ambient pressure. The reaction conditions were at 5 mM **A4**, 500 mM **D8**, 15 % (v/v) DMSO and 100 μM triple mutant. To monitor the reaction progress, aliquot (typically 10 μL) of the reaction mixture was taken at predetermined reaction times and then mixed with 190 μL of 4.4 % (v/v) $HClO_4$ solution. After centrifugation, the resulting supernatant was subjected to chiral HPLC analysis of the produced (*S*)-**D4**.

Preparative-scale synthesis of (*S*)-D4

To determine the optimal amount of DMSO for preparative-scale synthesis of (*S*)-**D4**, small-scale reactions were carried out at 100 mM **A4**, 500 mM **D8**, 0.1 mM PLP and 10 μM triple mutant in the presence of 10-50 % (v/v) DMSO. The reaction volume was 1 mL. All the enzyme reactions were conducted at pH 9 (50 mM Tris buffer) and 37 °C under ambient pressure.

Preparative-scale synthesis of (*S*)-**D4** was performed in a 100 mL reactor charged with 50 mL reaction mixture containing 50 mM **A4**, 500 mM **D8**, 0.1 mM PLP, 100 μM triple mutant, 30 % (v/v) DMSO and 50 mM Tris buffer (pH 9). The preparative-scale reaction was carried out at 37 °C and 0.6 bar under mild magnetic stirring. At predetermined reaction times, aliquot of the reaction mixture (typically 10 μL) was taken and mixed with 190 μL of 4.4 % (v/v) $HClO_4$ solution. The reaction progress was monitored by HPLC analysis of produced (*S*)-**D4**. To measure the residual activities of the triple mutant during the reaction, activity assay was conducted by adding aliquot of the reaction mixture to an assay solution containing 10 mM (*S*)-**D1**, 10 mM **A6** and 50 mM potassium phosphate buffer (pH 7.0). Produced **A1** was analyzed by HPLC.

Product isolation was carried out using cation-exchange chromatography. The pH of the reaction mixture was adjusted to 1.0 by adding 5 N HCl and the protein precipitate was removed by centrifugation (10000×g, 20 min), followed by filtration through a glass-fritted filter funnel. The resulting filtrate was loaded on a glass column packed with Dowex 50WX8 cation-exchange resin (40 g). Washing and elution were carried out by sequential loading of water (200 mL) and then 10 % (v/v) ammonia solution (840 mL). The eluates were collected and then (*S*)-**D4** was extracted with *n*-hexane (600 mL). The resulting extractant pool was evaporated at 50 °C and 0.45 bar, yielding clear liquid of (*S*)-**D4**. The isolated (*S*)-**D4** was structurally characterized by ^1H NMR, ^{13}C NMR and LC/MS. Details of the structural characterization are described in the

Supporting Information.

HPLC analysis

HPLC analyses were carried out on an Alliance system (Waters Co.) or a 1260 Infinity system (Agilent Technologies). Quantitative analyses of ketones were performed using a Symmetry C18 column (Waters Co.). Chiral analyses of amines were carried out using a Crownpak CR-I(+) column (Daicel Co.). Details of the HPLC analysis are described in the Supporting Information.

Acknowledgements

This work was funded by the National Research Foundation of Korea under the Basic Science Research Program (2016R1A2B4008470). Dr. S.-W. Han was financially supported by Initiative for Biological Function & Systems under the BK21 PLUS program of Korean Ministry of Education. We are grateful to the technical work of Saerom Park.

References

[1] a) T. C. Nugent, *Chiral Amine Synthesis: Methods, Developments and Applications*, Wiley-VCH, Weinheim, **2010**; b) U. T. Bornscheuer, G. W. Huisman, R. J. Kazlauskas, S. Lutz, J. C. Moore, K. Robins, **Nature 2012**, *484*, 185-194; c) M. Breuer, K. Ditrich, T. Habicher, B. Hauer, M. Kesseler, R. Sturmer, T. Zelinski, *Angew. Chem. Int. Ed*. **2004**, *43*, 788-824; d) V. Gotor-Fernández, V. Gotor, *Curr. Opin. Drug Discov. Devel.* **2009**, *12*, 784-797.

[2] T. C. Nugent, M. El-Shazly, *Adv. Synth. Catal*. **2010**, *352*, 753-819.

[3] D. Ghislieri, N. J. Turner, *Top. Catal*. **2014**, *57*, 284-300.

[4] a) M. S. Malik, E. S. Park, J. S. Shin, *Appl. Microbiol. Biotechnol.* **2012**, *94*, 1163-1171; b) R. C. Simon, N. Richter, E. Busto, W. Kroutil, *ACS Catal*. **2014**, *4*, 129-143; c) F. Guo, P. Berglund, *Green Chem*. **2017**, *19*, 333-360; d) S. A. Kelly, S. Pohle, S. Wharry, S. Mix, C. C. R. Allen, T. S. Moody, B. F. Gilmore, *Chem. Rev*. **2018**, *118*, 349-367.

[5] a) C. K. Savile, J. M. Janey, E. C. Mundorff, J. C. Moore, S. Tam, W. R. Jarvis, J. C. Colbeck, A. Krebber, F. J. Fleitz, J. Brands, P. N. Devine, G. W. Huisman, G. J. Hughes, *Science* **2010**, *329*, 305-309; b) K. S. Midelfort, R. Kumar, S. Han, M. J. Karmilowicz, K. McConnell, D. K. Gehlhaar, A. Mistry, J. S. Chang, M. Anderson, A. Villalobos, J. Minshull, S. Govindarajan, J. W. Wong, *Protein Eng. Des. Sel*. **2013**, *26*, 25-33; c) A. Nobili, F. Steffen-Munsberg, H. Kohls, I. Trentin, C. Schulzke, M. Höhne, U. T. Bornscheuer, *ChemCatChem* **2015**, *7*, 757-760; d) S. W. Han, J. Kim, H. S. Cho, J. S. Shin, *ACS Catal*. **2017**, *7*, 3752-3762; e) S. W. Han, E. S. Park, J. Y. Dong, J. S. Shin, *Adv. Synth. Catal*. **2015**, *357*, 1732-1740; f) K. E. Cassimjee, M. S. Humble, H. Land, V. Abedi, P. Berglund, *Org. Biomol. Chem*. **2012**, *10*, 5466-5470.

[6] a) K. Hirotsu, M. Goto, A. Okamoto, I. Miyahara, *Chem. Rec*. **2005**, *5*, 160-172; b) M. D. Toney, *Arch. Biochem. Biophys*. **2014**, *544*, 119-127.

[7] a) J. S. Shin, B. G. Kim, *J. Org. Chem*. **2002**, *67*, 2848-2853; b) U. Kaulmann, K. Smithies, M. E. B. Smith, H. C. Hailes, J. M. Ward, *Enzyme Microb. Technol*. **2007**, *41*, 628-637; c) B. M. Nestl, S. C. Hammer, B. A. Nebel, B. Hauer, *Angew. Chem. Int. Ed*. **2014**, *53*, 3070-3095.

[8] a) M. Voss, D. Das, M. Genz, A. Kumar, N. Kulkarni, J. Kustosz, P. Kumar, U. T. Bornscheuer, M. Höhne, *ACS Catal*. **2018**, *8*, 11524-11533; b) M. S. Weiß, I. V. Pavlidis, P. Spurr, S. P. Hanlon, B. Wirz, H. Iding, U. T. Bornscheuer, *ChemBioChem* **2017**, *18*, 1022-1026; c) I. V. Pavlidis, M. S. Weiß, M. Genz, P. Spurr, S. P. Hanlon, B. Wirz, H. Iding, U. T. Bornscheuer, *Nat. Chem*. **2016**, *8*, 1076-1082.

[9] a) K. E. Cassimjee, B. Manta, F. Himo, *Org. Biomol. Chem.* **2015**, *13*, 8453-8464; b) F. Steffen-Munsberg, C. Vickers, A. Thontowi, S. Schätzle, T. Tumlirsch, M. S. Humble, H. Land, P. Berglund, U. T. Bornscheuer, M. Höhne *ChemCatChem* **2013**, *5*, 150-153; c) M. Höhne, S. Schätzle, H. Jochens, K. Robins, U. T. Bornscheuer, *Nat. Chem. Biol*. **2010**, *6*, 807-813; d) E. S. Park, J. Y. Dong, J. S. Shin, *Appl. Microbiol. Biotechnol.* **2014**, *98*, 651-660; e) E. S. Park, S. R. Park, S. W. Han, J. Y. Dong, J. S. Shin, *Adv. Synth. Catal*. **2014**, *356*, 212-220; f) E.-S. Park, M. Kim, J.-S. Shin, *Appl. Microbiol. Biotechnol*. **2012**, *93*, 2425-2435.

[10] D. Koszelewski, K. Tauber, K. Faber, W. Kroutil, *Trends Biotechnol*. **2010**, *28*, 324-332.

[11] a) A. Nobili, F. Steffen-Munsberg, H. Kohls, I. Trentin, C. Schulzke, M. Höhne, U. T. Bornscheuer, *ChemCatChem* **2015**, *7*, 757-760; b) M. Genz, O. Melse, S. Schmidt, C. Vickers, M. Dörr, T. van den Bergh, H.-J. Joosten, U. T. Bornscheuer, *ChemCatChem* **2016**, *8*, 3199-3202.

[12] V. N. Malashkevich, J. J. Onuffer, J. F. Kirsch, J. N. Jansonius, *Nat. Struct. Mol. Biol*. **1995**, *2*, 548-553.

[13] a) S. W. Han, E. S. Park, J. Y. Dong, J. S. Shin, *Adv. Synth. Catal*. **2015**, *357*, 2712-2720; b) S. W. Han, E. S. Park, J. Y. Dong, J. S. Shin, *Appl. Environ. Microbiol*. **2015**, *81*, 6994-7002.

[14] A. W. H. Dawood, M. S. Weiß, C. Schulz, I. V. Pavlidis, H. Iding, R. O. M. A. de Souza, U. T. Bornscheuer, *ChemCatChem* **2018**, *10*, 3943-3949.

[15] A. Iwasaki, K. Matsumoto, J. Hasegawa, Y. Yasohara, *Appl. Microbiol. Biotechnol*. **2012**, *93*, 1563-1573.

[16] E. S. Park, J. Y. Dong, J. S. Shin, *Org. Biomol. Chem* **2013**, *11*, 6929-6933.

[17] C. Rausch, A. Lerchner, A. Schiefner, A. Skerra, *Proteins* **2013**, *81*, 774-787.

10.1002/adsc.201900184

FULL PAPER

Combinatorial Mutation Analysis of ω-Transaminase to Create an Engineered Variant Capable of Asymmetric Amination of Isobutyrophenone

Adv. Synth. Catal. **Year**, *Volume*, Page – Page

Hong-Gon Kim, Sang-Woo Han and Jong-Shik Shin*